0026-895X/04/6506-1375–1385$20.00
MOLECULAR PHARMACOLOGY
Vol. 65, No. 6
3172/1151021
Mol Pharmacol 65:1375–1385, 2004
Printed in U.S.A.

Mutations of Charged Amino Acids in or near the Transmembrane Helices of the Second Membrane Spanning Domain Differentially Affect the Substrate Specificity and Transport Activity of the Multidrug Resistance Protein MRP1 (ABCC1)

Anass Haimeur, Gwenaëlle Conseil, Roger G. Deeley, and Susan P.C. Cole

Cancer Research Laboratories, Queen's University, Kingston, Ontario, Canada

Received December 19, 2003; accepted February 23, 2004

This article is available online at http://molpharm.aspetjournals.org

ABSTRACT

Multidrug resistance protein 1 (MRP1) belongs to the ATP-binding cassette superfamily of transport proteins. In addition to drugs, MRP1 mediates the active transport of many conjugated and unconjugated organic anions. MRP1 consists of two membrane-spanning domains (MSD2 and MSD3) each followed by a nucleotide binding domain plus a third NH_2-terminal MSD1. MSD2 contains transmembrane (TM) helices 6 through 11, and previously, we identified two charged residues in TM6 as having important but markedly different roles in MRP1 transport activity and substrate specificity by characterizing mutants containing nonconservative substitutions of Lys^{332} and Asp^{336}. We have now extended these studies and found that the same-charge TM6 mutant K332R, like the nonconservatively substituted Lys^{332} mutants, exhibits a selective decrease in leukotriene C_4 (LTC_4) transport, associated with substantial changes in both K_m and V_{max} and LTC_4 binding. The overall organic anion transport activity of the same-charge mutant of Asp^{336} (D336E) also remained very low, as observed for D336R. In addition, nonconservative substitutions of TM6-associated Lys^{319} and Lys^{347} resulted in a selective decrease in GSH transport. Of eight other charged residues in or proximal to TM7 to TM11 that were investigated, nonconservative substitutions of three of them [Lys^{396} (TM7), Asp^{436} (TM8), and Arg^{593} (TM11)] caused a substantial and global reduction in transport activity. However, unlike TM6 Asp^{336}, wild-type transport activity could be re-established in these MRP1 mutants by conservative substitutions. We conclude that MSD2-charged residues in or proximal to TM6, TM7, TM8, and TM11 play critical but differential roles in MRP1 transport activity and substrate specificity.

MRP1 is a 190-kDa multidrug resistance protein that belongs to subfamily C of the ABC transporter superfamily and is often overexpressed in drug-resistant tumor cell lines (Haimeur et al., 2004). It is also expressed in a wide variety of human tumors and normal tissues. In vitro studies using membrane vesicles have demonstrated that MRP1 can actively transport a wide variety of structurally diverse compounds ranging from complex heterocyclic natural products and chemotherapeutic agents, such as vincristine, doxorubicin and the folate antagonist methotrexate, to arsenical and antimonial oxyanions (Borst et al., 2000; Deeley and Cole, 2003; Haimeur et al., 2004). MRP1 has also been shown to be an efficient ATP-dependent transporter of various conjugated organic anions, including a mediator of inflammation, the cysteinyl leukotriene LTC_4, and the glucuronide- and sulfate-conjugated estrogens $E_2 17\beta G$ and $E_1 3SO_4$. To transport unconjugated drugs such as vincristine, MRP1 requires the presence of GSH, which seems to be cotransported with the drug (Loe et al., 1998; Mao et al., 2000). MRP1 also transports small hydrophobic peptides (de Jong et al., 2001). Thus, the range of substrates that can be transported by MRP1, at least in vitro, is very broad.

The two basic structural elements of all known ABC transporters are a nucleotide-binding domain (NBD) and a hydrophobic region typically containing six transmembrane (TM)

This work was supported by grant MOP-10519 from the Canadian Institutes of Health Research. A.H. and G.C. are recipients of Canadian Institutes of Health Research Postdoctoral Fellowships. R.G.D. is the Stauffer Research Professor of Queen's University. S.P.C.C. is the Canada Research Chair in Cancer Biology and Senior Scientist of Cancer Care Ontario.

ABBREVIATIONS: MRP1, multidrug resistance protein 1; ABC, ATP-binding cassette; CFTR, cystic fibrosis transmembrane conductance regulator; LTC_4, leukotriene C_4; $E_2 17\beta G$, 17β-estradiol 17-(β-D-glucuronide); MSD, membrane-spanning domain; TM, transmembrane; NBD, nucleotide binding domain; $E_1 3SO_4$, estrone 3-sulfate; GFP, green fluorescence protein; MTX, methotrexate; kb, kilobase; HEK, human embryonic kidney; GSH, glutathione.

α-helices, which together constitute a membrane-spanning domain (MSD) (Higgins, 1992). The most common structure of ABC transporters is one with four domains: two MSDs and two NBDs. However, MRP1 and several other members of the ABCC transport protein family have an additional NH_2-terminal MSD with five TM segments and an extracytosolic NH_2 terminus (Hipfner et al., 1997; Raab-Graham et al., 1999; Konig et al., 2003). Thus, most computer algorithms for predicting secondary structures of integral membrane proteins favor a structure in which human MRP1 possesses 17 TM α-helices configured 5 + 6 + 6 in its three MSDs, respectively (Fig. 1).

The role that the MSDs of MRP1 play in determining its transport activity and substrate specificity has recently been the subject of considerable investigation, primarily by structure-function studies using site-directed mutagenesis. These studies have shown that mutation of individual aromatic, polar, and charged amino acids in each of the three MSDs can affect the recognition and transport of one or several substrates in different ways (Ito et al., 2001a; Zhang et al., 2001, 2002, 2003; Koike et al., 2002; Haimeur et al., 2002; Yang et al., 2002; Leslie et al., 2003b). In one study, we showed that nonconservative substitutions of three charged amino acids predicted to cluster within an arc of approximately 100° on the same face of TM6 of MSD2 (Lys^{332}, His^{335}, and Asp^{336}) had strikingly different effects on MRP1 transport activity and substrate specificity (Fig. 1) (Haimeur et al., 2002). Thus, Lys^{332} and, to a certain extent, His^{335} were found to be critical for the binding and transport of LTC_4 and GSH, whereas mutation of these residues had little or no impact on the transport of other organic anions. In contrast, nonconservative substitutions of Asp^{336} showed no such substrate selectivity because mutation of this acidic residue to either an oppositely charged or neutral amino acid essentially eliminated MRP1 transport activity altogether (Haimeur et al., 2002). We have also shown that the naturally occurring MSD2 mutation Arg^{433}→Ser, predicted to be located in the fourth cytoplasmic loop in close proximity to the membrane interface of TM8, causes a selective decrease in LTC_4 and E_13SO_4 transport efficiency (Conrad et al., 2002). Together, these studies show that charged amino acids in or proximal to MSD2 can be important for both the substrate specificity and overall transport activity of MRP1.

In the present study, we extended our investigations of charged amino acids in MSD2 by first creating additional mutations of TM6 Lys^{332} and Asp^{336} to address the question

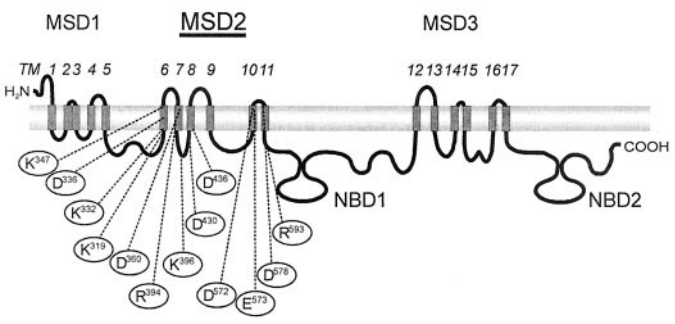

Fig. 1. Topological model of MRP1 based on hydropathy analyses showing the approximate location of charged amino acids in and proximal to the transmembrane helices (TM6–TM11) of MSD2 that were mutated in this study. The seventeen TM helices and two NBDs of MRP1 are also indicated.

of whether the charge and/or physical volume of the amino acid side chain is important for substrate transport by MRP1 and whether bonding interactions between these two residues in TM6 exist. In addition, we investigated the functional consequences of mutating each of the remaining five positively (Lys^{319}, Lys^{347}, Arg^{394}, Lys^{396}, and Arg^{593}) and six negatively (Asp^{360}, Asp^{430}, Asp^{436}, Asp^{572}, Glu^{573}, and Asp^{578}) charged amino acids that are predicted by hydropathy analyses using the algorithm of Eisenberg et al. (1984) and the PredictProtein neural network system (Rost et al., 1996) to be in or near the TM helices of this domain (Hipfner et al., 1997) (Fig. 1). We found that nonconservative and conservative mutations of 8 of the 13 MSD2-charged residues examined differentially affected MRP1 expression, transport activity, and/or substrate specificity. Thus, our findings demonstrate the following: 1) both the charge and side chain volume of TM6 Lys^{332} are critical for binding/transport of LTC_4 and GSH but not other organic anions; 2) Lys^{319} and Lys^{347} proximal to TM6 seem to contribute selectively to GSH transport activity; 3) Asp^{430} is required for stable MRP1 expression in mammalian cells; and 4) Asp^{336} (TM6), Lys^{396} (TM7), Asp^{436} (TM8), and Arg^{593} (TM11) are important for overall MRP1 transport activity; however, activity is retained when these residues are replaced with same-charge amino acids, with the notable exception of TM6 Asp^{336}.

Materials and Methods

Materials. [14,15 (N)-^{3}H]LTC_4 (115.3 Ci mmol^{-1}) was purchased from Amersham Biosciences Inc. (Piscataway, NJ). [6,7-^{3}H]$E_217\beta G$ (55 Ci mmol^{-1}), [6,7 (N)-^{3}H]estrone 3-sulfate, and [glycine-2-^{3}H]GSH (40–44.8 Ci mmol^{-1}) were purchased from PerkinElmer Life and Analytical Sciences (Boston, MA). [3′,5′,7′-^{3}H (N)]Methotrexate sodium salt (17 Ci mmol^{-1}) was from Moravek Biochemicals (Brea, CA). LTC_4 was purchased from CalBiochem (San Diego, CA), and nucleotides, GSH, acivicin, $E_217\beta G$, and dithiothreitol were purchased from Sigma Chemical Co. (St. Louis, MO).

Vector Construction and Site-Directed Mutagenesis. The MRP1 expression vector pcDNA3.1(−)-$MRP1_K$ has been described previously (Ito et al., 2001a). Site-directed mutagenesis was performed using the QuikChange site-directed mutagenesis kit (Stratagene, La Jolla, CA). The template for mutagenesis was prepared by cloning a 1.88-kb BamHI-SphI fragment from pcDNA3.1(−)-$MRP1_K$ (containing nucleotides 840-2720 of the MRP1 sequence encoding amino acids 240–907) into pGEM-3Z (Promega, Madison, WI). Mutations were generated according to the manufacturer's instructions. The sequences of the individual sense strands (with the corresponding amino acid changes indicated in parentheses, the altered codons underlined, and silent mutations introducing new restriction sites italicized) were as follows: K(D)332K, 5′-G AGC TTC TTC TTC AAG GCC ATC CAC GAC CTG-3′; K332R, 5′-G AGC TTC TTC TTC AGG GCC ATC CAC GAC CTG-3′; D(K)336E, 5′-C AAG GCC ATC CAC GAG CT*C* ATG ATG TTT TCC-3′; D336K, 5′-C AAG GCC ATC CAC AAG CT*T* ATG ATG TTT TCC-3′; K332D/D336K, 5′-GC TTC TTC TTC GAC GCC ATC CAC AAA CTG ATG ATG-3′; K319D, 5′-G TTT AAG GTG TTA TAC GAC AC*G* TTT GGG CCC-3′; K347D, 5′-GGG CCG CAG ATA TTA GAC TTG CTC ATC AAG-3′; K347L, 5′-GGG CCG CA*A* ATC TTA CTT TTG CTC ATC AAG-3′; D360K, 5′-GAC ACG AAG GCG CCA AAG TGG CAG GGC TAC-3′; R394D, 5′-C GTC AGT GGC ATG GAG ATC AAG ACC GCT GTC-3′; R394I, 5′-C GTC AGT GGC ATG ATC ATC AAG ACC GCT GTC-3′; K396E, 5′-GT GGC ATG AGG ATC GAG ACC GCT GTC ATT GGG-3′; K396I, 5′-GT GGC ATG AGG ATC ATC ACC GCT GTC ATT GGG-3′; K(E)396R, 5′-GGC ATG AGG ATC AGG ACC GCT GTC ATT GGG GC-3′; D430K, 5′-C AAC CTC ATG TCT GTG AAG GCT CAG AGG

TTC-3′; D430R, 5′-C AAC CTC ATG TCT GTG CGC GCT CAG AGG TTC-3′; D436K, 5′-C GCT CAG AGG TTC ATG AAG TTG GCC ACG TAC-3′; D(K)436E, 5′-C GCT CAG AGG TTC ATG GAA TTA GCC ACG TAC-3′; D572R, 5′-C TAC GTG ACC ATT CGC GAG AAC AAC ATC CTG G-3′; E573R, 5′-C GTG ACC ATT GAC CGG AAC AAC ATC CTG GAT G-3′; D578R, 5′-G AAC AAC ATC CTG CGG GCC CAG ACA GCC TTC G-3′; R593E, 5′-G GCC TTG TTC AAC ATC CTC GAG TTT CCC CTG AAC-3′; R593L, 5′-G GCC TTG TTC AAC ATC CTC CTG TTT CCC CTG AAC-3′; R(E)593K, 5′-GCC TTG TTC AAC ATC CTT AAG TTT CCC CTG AAC-3′.

The presence of the mutations was confirmed by sequencing and/or diagnostic restriction enzyme digests as appropriate. Mutant MRP1 cDNAs were then digested with BamHI and Bsu36I to obtain a 1-kb fragment containing the altered sequence, which was used to replace the corresponding fragment in the wild-type pcDNA3.1(−)-$MRP1_K$ plasmid. After cloning, the inserts were again sequenced to confirm the presence of the mutation. For selected mutants, MRP1-green fluorescent protein (GFP) fusion constructs were generated by replacing the 1-kb BamHI/Bsu36I fragment in a pcDNA3.1(−)-$MRP1_k$-GFP construct with the comparable fragment containing the desired mutation. Confocal microscopy was carried out as described previously (Haimeur et al., 2002).

Transfections with MRP1 Expression Vectors. Wild-type and mutant pcDNA3.1(−)-MRP1 expression vectors were transfected into SV40-transformed human embryonic kidney cells (HEK 293T). In brief, approximately 10×10^6 cells were seeded in 150-mm plates, and 24 h later, DNA (16 μg) was added using FuGENE6 (Roche Diagnostics, Laval, PQ, Canada) according to the manufacturer's instructions. After 72 h, the HEK 293T cells were harvested, and membrane vesicles prepared as described previously (Haimeur et al., 2002). Untransfected cells or cells transfected with empty vector, and vector containing wild-type MRP1 cDNA were included as controls in all experiments. Levels of wild-type and mutant MRP1 proteins were determined by immunoblotting as described below.

Measurement of MRP1 Protein Levels in Transfected Cells. The expression levels of wild-type and mutant MRP1 proteins were determined by immunoblot analysis of whole-cell lysates and membrane vesicles from transfected cells essentially as described using the human MRP1-specific murine MAb QCRL-1 (Hipfner et al., 1996) and the Renaissance chemiluminescence detection system (PerkinElmer Life and Analytical Sciences). Relative levels of MRP1 expression were estimated by densitometric analysis using a Chemi-Imager 4000 (Alpha Innotech, San Leandro, CA). Equal loading of proteins was confirmed by amido black staining of the membranes.

MRP1-Mediated Transport of ^{3}H-Labeled Substrates by Membrane Vesicles. Preparation of membrane vesicles from transfected HEK 293T cells has been described previously (Haimeur et al., 2002), and ATP-dependent vesicular uptake of ^{3}H-labeled substrates by the membrane vesicles was measured using a rapid filtration technique also as described previously (Haimeur et al., 2002). In brief, LTC_4 transport assays were performed at 23°C in a 50-μl reaction containing 50 nM LTC_4 (40 nCi), 4 mM AMP or ATP, 10 mM $MgCl_2$, creatine phosphate (10 mM), creatine kinase (100 $\mu g \cdot ml^{-1}$), and 2 μg of vesicle protein. Uptake was stopped at selected times by rapid dilution in ice-cold buffer, and then the incubation mixture was filtered through glass fiber (type A/E) filters that had been presoaked in transport buffer. Radioactivity was quantified by liquid scintillation counting. All data were corrected for the amount of [^{3}H]LTC_4 that remained bound to the filter, which was usually <10% of the total radioactivity. Transport in the presence of AMP was subtracted from transport in the presence of ATP to determine ATP-dependent LTC_4 uptake. All transport assays were carried out in triplicate, and results expressed as means (± S.D.).

Vesicular uptake of $E_2 17\beta G$ was measured in a similar fashion, except that membrane vesicles (2 μg of protein) were incubated at 37°C in a total reaction volume of 50 μl containing [^{3}H]$E_2 17\beta G$ (400 nM; 40 nCi) and components as described for [^{3}H]LTC_4 transport. GSH-stimulated ATP-dependent transport of $E_1 3SO_4$ into membrane vesicles was measured as described above for [^{3}H]$E_2 17\beta G$, except that the initial substrate concentration was 300 nM (200 nCi) [^{3}H]$E_1 3SO_4$, and the reaction volume was 60 μl containing 3 mM GSH and 10 mM dithiothreitol and 2.5 μg of vesicle protein. GSH uptake was also measured by rapid filtration with membrane vesicles (20 μg of protein) incubated at 37°C for 20 min in a 60-μl reaction volume with 100 μM [^{3}H]GSH (300 nCi per reaction) and 30 μM apigenin (Leslie et al., 2003a). To minimize GSH catabolism by γ-glutamyltranspeptidase during transport, membranes were preincubated in 0.5 mM acivicin for 10 min at 37°C before measuring [^{3}H]GSH uptake. MTX uptake was also measured as described previously (Haimeur et al., 2002). Assays were carried out at 37°C in a 60-μl reaction volume containing [^{3}H]MTX (100 μM; 200 nCi), membrane vesicles (10 μg of protein), and other components as described above. Uptake was stopped after 20 min by rapid dilution in ice-cold buffer and processed as before.

Kinetic Analysis of ATP-Dependent [^{3}H]LTC_4 and [^{3}H]$E_2 17\beta G$ Uptake. K_m and V_{max} values of ATP-dependent LTC_4 transport by membrane vesicles (2.5 μg of protein) were determined by measuring initial rates of uptake at eight different [^{3}H]LTC_4 concentrations (10–1000 nM) for 1 min at 23°C. For kinetics of [^{3}H]$E_2 17\beta G$ uptake, substrate concentrations ranged from 0.25 to 25 μM, and vesicles were incubated for 1 min at 37°C in 50 μl of transport buffer containing components as described above. Data were analyzed using Prism software (GraphPad Software Inc., San Diego, CA), and kinetic parameters determined by linear regression analyses and Michaelis-Menten analysis.

Photolabeling of MRP1 with [^{3}H]LTC_4. Wild-type and mutant MRP1 membrane proteins were photolabeled with [^{3}H]LTC_4 essentially as described previously (Loe et al., 1996). In brief, membrane vesicles enriched for wild-type and mutant MRP1 cDNAs (50 μg of protein in 50 μl) were incubated with [^{3}H]LTC_4 (0.5 μCi; 200 nM) at room temperature for 30 min and then frozen in liquid nitrogen. Samples were then alternately irradiated at 312 nm for 1 min using a CL-1000 Ultraviolet Crosslinker (DiaMed, Mississauga, ON, Canada) and snap-frozen in liquid N_2 10 times. Radiolabeled proteins (50 μg) were resolved by SDS-polyacrylamide gel electrophoresis. The gel was processed for autoradiography and exposed to Kodak X-Omat film (Eastman Kodak, Rochester, NY) at −70°C.

Results

MRP1 Expression Levels of MSD2 Mutants in Transfected HEK Cells. To investigate whether charged amino acids predicted to be located in or near the TM α-helices of MSD2 (TM6–TM11) are important for MRP1 function, we first mutated them, singly and in one case in combination, to an oppositely charged residue and, in several cases, to a nonpolar neutral and/or same-charge residue (Fig. 1). These MSD2 mutants were cloned into the pcDNA3.1(−) expression vector and expressed in HEK 293T cells as described previously (Haimeur et al., 2002). The expression levels of the mutant MRP1 proteins were determined by immunoblot analysis of membrane vesicles prepared from the transfected cells, and in all cases but one, a single band of 190 kDa corresponding to MRP1 was detected (Fig. 2). The exception was the Asp^{430} mutant D430K which, like endogenous MRP1 in vector control membrane vesicles, was undetectable under the conditions used. Densitometric analysis showed that the levels of the expressed MRP1 mutants were comparable (80–120%) to wild-type MRP1, indicating that mutations of charged amino acids proximal to MSD2 (with the exception of Asp^{430}), did not significantly affect the biogenesis of MRP1. Comparable results were observed in immunoblots of whole-cell lysates of the transfected cells (data not shown).

Substitution of Lys^{332}, Asp^{336}, Lys^{319}, and Lys^{347} in or near TM6. We showed previously that nonconservative substitutions of Lys^{332} with either Asp (K332D) or Leu (K332L) led to a selective loss of transport of GSH and the GSH conjugate, LTC_4 (Haimeur et al., 2002). LTC_4 binding was also abrogated in these mutants as indicated by photolabeling and competition experiments. When the Asp residue of the K332D mutant was mutated back to the wild-type Lys residue to create K(D)332K, LTC_4 and GSH transport was restored as expected (Fig. 3, A and B). To test whether the charge and/or steric properties (side-chain volume) of Lys^{332} were important for the substrate selective loss of transport activity, Lys^{332} was also replaced with Arg to create the same-charge mutant K332R. Unlike the K332D mutant, the conservatively substituted K332R had a significant level of LTC_4 transport activity (approximately 40% of wild-type MRP1 levels). These results indicate that the charge and, to some extent, the molecular volume of the Lys^{332} side chain are important for LTC_4 transport by MRP1. Analysis of kinetic parameters showed that the decrease in LTC_4 transport by the same-charge K332R mutant was largely caused by a decrease in its apparent uptake affinity for LTC_4 (K_m = 552 nM versus 115 nM for wild-type MRP1), leading to an overall 6-fold decrease in LTC_4 transport efficiency (V_{max}/K_m = 0.2 versus 1.2 for wild-type MRP1) (Table 1).

To determine whether [^{3}H]$E_2$17βG transport by the like-

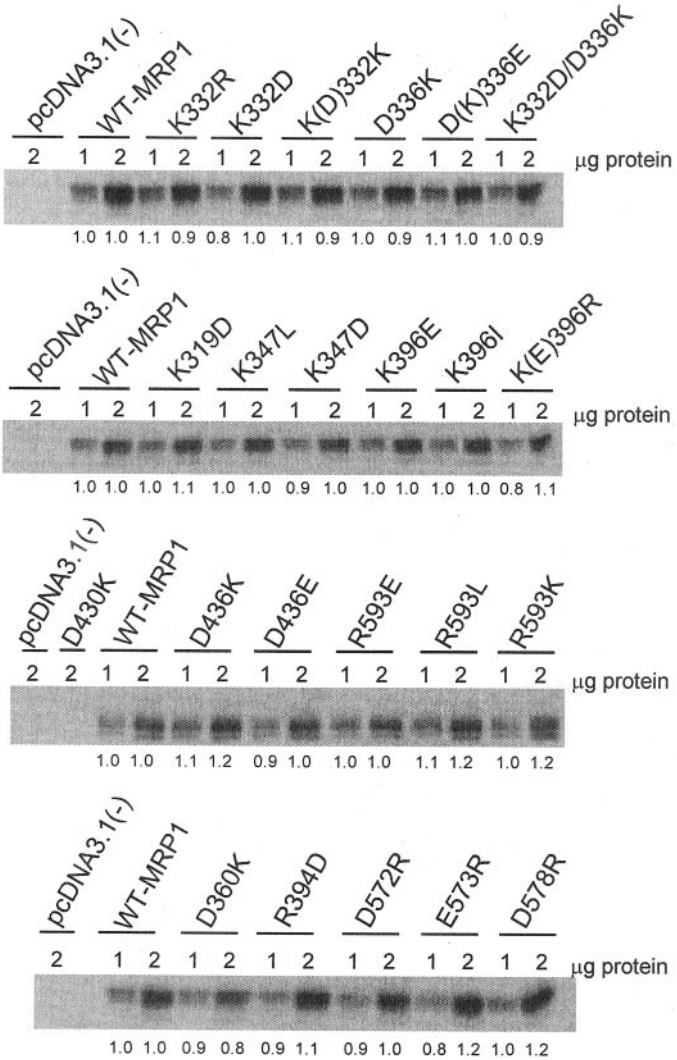

Fig. 2. Immunoblot of MRP1 mutants containing substitutions of charged amino acids in or proximal to MSD2. Membrane vesicles (1 and 2 μg of protein) prepared from HEK 293T cells transfected with empty vector [pcDNA3.1(−)], wild-type (WT-MRP1), and the indicated mutant MRP1 cDNAs were immunoblotted with MAb QCRL-1. Relative levels of MRP1 protein expression were estimated by densitometry and are indicated below each blot; equal protein loading of the wells of the gel was confirmed by amido black staining of the membrane (results not shown). Results shown are representative of MRP1 expression levels found in membrane vesicles from at least three independent transfections.

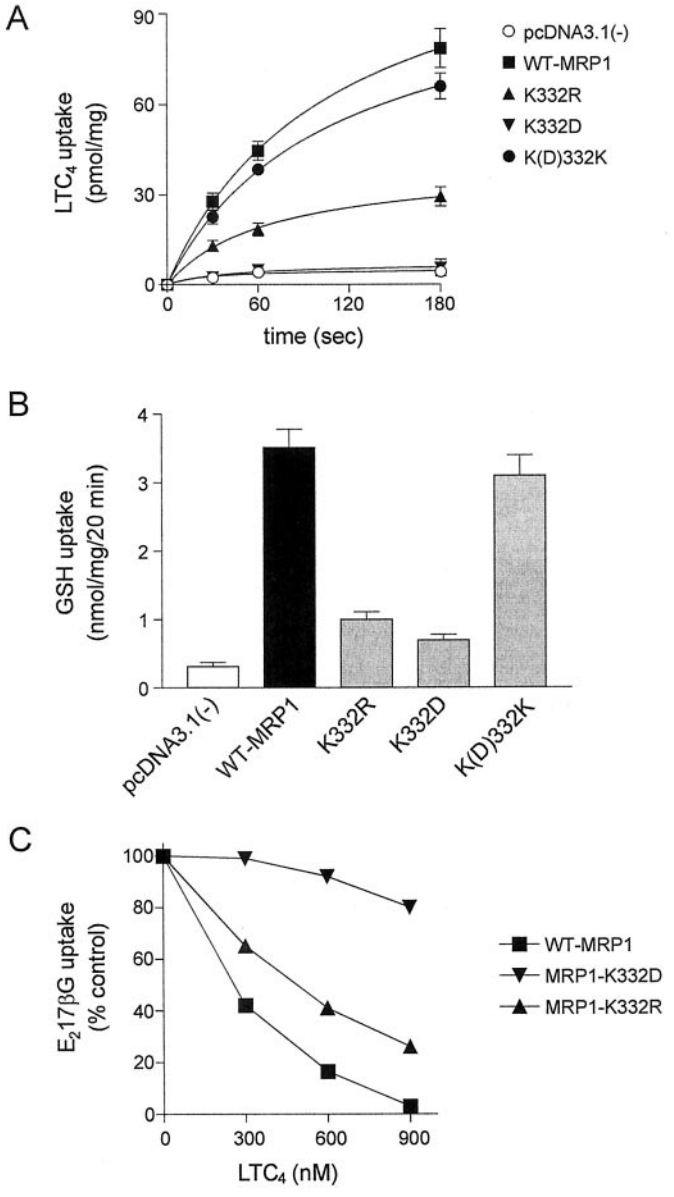

Fig. 3. ATP-dependent ^{3}H-labeled organic anion uptake by MRP1 TM6 mutants containing substitutions of Lys^{332}. A, time course of [^{3}H]LTC_4 uptake by wild-type MRP1 (■), mutants K332D (▼), K(D)332K (●), K332R (▲), and empty pcDNA3.1(−) vector control (○). B, [^{3}H]GSH uptake at 20 min by wild-type MRP1 (■) and mutants K332R, K332D, and K(D)332K (▨), and empty pcDNA3.1(−) vector control (□). C, [^{3}H]$E_2$17βG uptake at 1 min by wild-type (WT) MRP1 (■) and mutants K332D (▼) and K332R (▲) was measured in the presence of three different concentrations (300, 600, and 900 nM) of LTC_4. Results shown are means (± S.D.) of triplicate determinations in a single experiment. Relative MRP1 protein expression levels in the membrane vesicles were as shown in Fig. 2. Similar results were obtained in at least two additional experiments using vesicles from independent transfections.

charge K332R mutant that retained some LTC_4 transport activity could still be inhibited by this conjugated leukotriene, the effect of LTC_4 on [^{3}H]$E_2$17βG uptake by K332R was determined. The dose-response curves shown in Fig. 3C indicate that LTC_4 had a greater inhibitory effect on $E_2$17βG uptake by the K332R mutant than by the K332D mutant, but this effect was significantly less (50–70%) than the effect of LTC_4 on $E_2$17βG uptake by wild-type MRP1. These relative levels of inhibition by LTC_4 are consistent with the relative levels of LTC_4 transport by these three MRP1 proteins.

The same-charge mutant K332R, like the K332D and K332L mutants described previously (Haimeur et al., 2002), exhibited transport levels of the conjugated estrogens $E_2$17βG and $E_1$3SO_4 and the antifolate MTX that were comparable with wild-type MRP1 (Table 2); however, GSH transport by K332R was very low compared with wild-type MRP1 and similar to that which we reported previously for the K332D/L mutants (Fig. 3B). Overall, these observations indicate the Lys residue at position 332 is strictly required for full LTC_4 and GSH transport activity but not for transport of other organic anions (i.e., $E_2$17βG, $E_1$3SO_4, and MTX).

In our earlier study, we showed that substitution of the negatively charged TM6 Asp^{336} residue with Arg or Leu essentially eliminated the transport of both conjugated and unconjugated MRP1 organic anion substrates (Haimeur et al., 2002). In the present study, Asp^{336} was replaced with Lys to create D336K, and a comparable global loss of transport activity was observed (Fig. 4A and Table 2). To test whether the charge of Asp^{336} or the steric bulk of its side chain was responsible for the functional importance of this amino acid, the Lys in the D336K mutant was replaced with Glu to create the like-charge mutant D(K)336E. In contrast to the like-charge K332R mutant in which LTC_4 transport activity was partially restored, the like-charge D(K)336E mutant remained essentially inactive. Thus, LTC_4 and GSH uptake by D(K)336E was decreased >80 and 90%, respectively, compared with wild-type MRP1 (Fig. 4A), and transport of three other MRP1 substrates was decreased by 55 to 75% (Table 2). These data show that both the charge and size of the side chain of the Asp residue at position 336 are critical for MRP1 activity.

We speculated previously that ion pairing might be occurring between K332 and D336 in TM6 because they are within approximately one turn of an α-helix from one another (Haimeur et al., 2002). To test this idea, the K332D/D336K double mutant in which these two residues were exchanged was created. If ion pairing was important (and the only interaction between these two residues), then this double mutant might be expected to have wild-type transport activity. However, as shown in Fig. 4B, LTC_4 transport by K332D/D336K was not detectable. Transport of other organic anions by this double mutant was also markedly reduced (Table 2). These findings indicate that even if Lys^{332} and Asp^{336} form an ion pair in the TM6 α-helix, additional bonding interactions of these two residues with other residues in MRP1 are required for full transport activity.

To further investigate the functional role of charged amino acids proximal to TM6, we also mutated Lys^{319} and Lys^{347}. Lys^{319} was replaced with Asp (K319D), and Lys^{347} was replaced with Asp (K347D) as well as Leu (K347L). The effects of mutating either Lys^{319} or Lys^{347} were similar and substrate-specific. Thus the ability of the K319D, K347D, and K347L mutants to transport GSH was reduced by approximately 50% (Fig. 4C), whereas the transport of four other substrates (LTC_4, $E_2$17βG, $E_1$3SO_4 and MTX) by these mutants remained comparable with wild-type MRP1 (Table 2). Thus, these two Lys residues seem particularly important for GSH transport by MRP1.

Substitution of Asp^{360}, Arg^{394}, and Lys^{396} near TM7. We next replaced three charged amino acids (Asp^{360}, Arg^{394}, and Lys^{396}) that are predicted to be near TM7, according to at least one hydropathy-based topological model of MRP1. Asp^{360} was replaced with an oppositely charged Lys residue (D360K), whereas Arg^{394} and Lys^{396} were substituted with Asp and Glu, respectively, to introduce the opposite charge (R394D and K396E) and with a nonpolar neutral amino acid (Ile) to eliminate charge (R394I and K396I).

Substitution of Asp^{360} or Arg^{394} with an oppositely charged amino acid had no effect on the transport of any of the five organic anion substrates tested (Table 2). Likewise, replacement of Arg^{394} with a neutral Ile had no effect on transport (data not shown). These data indicate that neither Asp^{360} nor Arg^{394} plays an important role in the transport mechanism

TABLE 1

Kinetic parameters of LTC_4 uptake by MRP1 MSD2 mutants containing substitutions of Lys^{332}, Lys^{396}, Asp^{436}, and Arg^{593}

Transfectants	K_m	V_{max}	V_{max}/K_m
	nM	*pmol/mg/min*	$\times 10^3$
Wild-type MRP1	115	135	1.2
K332R	552	137	0.2
K396E	448	62	0.1
K(E)396R	113	121	1.1
D436K	196	41	0.2
D(K)436E	126	150	1.2
R593E	464	56	0.1
R(E)593K	123	139	1.1

TABLE 2

Summary of organic anion transport activity of MRP1 mutants with substitutions of charged amino acids in and proximal to the TM helices (TM6–11) of MSD2

The values shown are means of triplicate determinations and are derived from this study (Figs. 3–7) and from Haimeur et al. (2002). For clarity, numbers have been rounded to the nearest 5%, and S.D. values (which were typically less than 10%) were omitted.

MRP1 Mutant	% Wild-Type MRP1 Transport Activity				
	LTC_4	GSH	$E_2$17βG	$E_1$3SO_4	MTX
TM6					
K332D	<10	<10	100	100	100
K332R	40	20	100	100	100
D336K	<10	<10	<10	15	45
D(K)336E	20	<10	25	25	45
K332D/D336K	<10	<10	30	25	50
K319D	100	50	100	100	100
K347D	100	45	100	100	100
TM7					
D360K	100	100	100	100	100
R394D	100	100	100	100	100
K396E	25	50	25	25	35
K(E)396R	100	100	100	100	100
TM8					
D436K	40	30	20	30	55
D(K)436E	100	100	100	100	100
ECL5/TM11					
D572R	100	100	100	100	100
E573R	100	100	100	100	100
D578R	100	100	100	100	100
R593E	35	30	<10	<10	40
R(E)593K	100	100	100	100	100

or substrate specificity of MRP1. In contrast, substitution of the nearby Lys^{396} residue with either an oppositely charged (K396E) or neutral (K396I) residue resulted in a substantial decrease in overall MRP1 transport activity (Fig. 5). Thus, LTC_4, $E_2 17\beta G$, and $E_1 3SO_4$ transport by the K396E and K396I mutants was reduced by 60 to 75% (Fig. 5, A-C) whereas GSH and MTX transport by these two mutants was reduced by approximately 50% (Fig. 5, D and E). Kinetic analyses indicated that both the apparent uptake affinity and the transport capacity of the K396E mutant for LTC_4 and $E_2 17\beta G$ were altered. In the case of LTC_4 transport, the

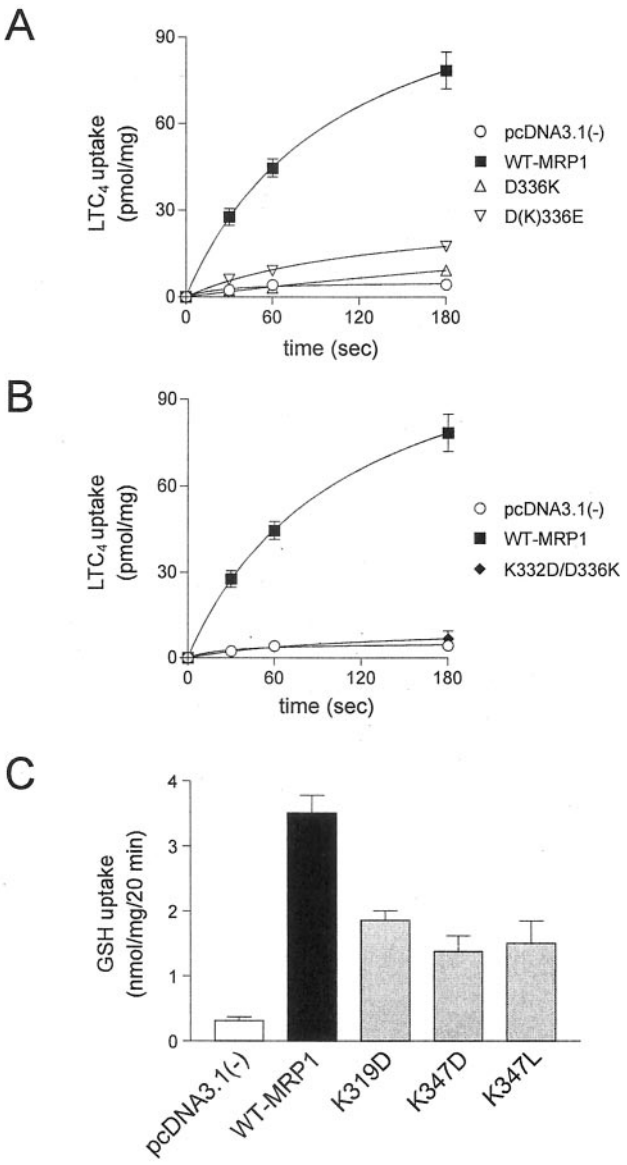

Fig. 4. ATP-dependent ^3H-labeled organic anion uptake by MRP1 mutants containing substitutions of charged amino acids in or proximal to TM6. A, time course of $[^3H]LTC_4$ uptake by wild-type MRP1 (■), mutants D336K (△), D(K)336E (▽), and empty pcDNA3.1(−) control (○). B, time course of $[^3H]LTC_4$ uptake by wild-type MRP1 (■), TM6 double mutant K332D/D336K (◆), and empty pcDNA3.1(−) vector control (○). C, apigenin-stimulated $[^3H]GSH$ uptake at 20 min by wild-type (WT) MRP1 (■), mutants K319D, K347D, and K347L (▨), and empty pcDNA3.1(−) vector control (□). Results shown are means (± S.D.) of triplicate determinations in a single experiment. Relative MRP1 protein expression levels in the membrane vesicles were as shown in Fig. 2. Similar results were obtained in at least two additional independent experiments.

K_m was increased 4-fold, whereas the V_{max} was reduced >2-fold, resulting in a 10-fold decrease in the transport efficiency of this substrate (Table 1). For $E_2 17\beta G$ transport, the K_m was increased 2-fold, while the V_{max} decreased 3-fold, resulting in 4.6-fold decrease in the overall transport efficiency of this substrate (Table 3).

To test whether the positive charge of the Lys^{396} side chain was the physical property critical for MRP1 transport function, the Glu in the K396E mutant was replaced with Arg to create the same-charge mutant K(E)396R. As shown in Fig. 5, uptake levels of all five organic anion substrates by the K(E)396R mutant were comparable with wild-type MRP1. The apparent K_m and V_{max} of K(E)396R for LTC_4 and $E_2 17\beta G$ transport were also similar to wild-type MRP1 (Tables 1 and 3). Thus, unlike Lys^{332} and Asp^{336} in TM6, in which both charge and side-chain volume were essential for transport activity, the presence of a positive charge alone at position 396 seems sufficient for wild-type MRP1 transport function.

Substitution of Asp^{430} and Asp^{436} in or near TM8. We previously showed that the naturally occurring $Arg^{433}\rightarrow Ser$ single nucleotide polymorphism proximal to the cytoplasmic end of TM8 resulted in a decrease in LTC_4 and $E_1 3SO_4$ transport and an increase in doxorubicin resistance (Conrad et al., 2002). In the present study, we investigated the effects of mutating the nearby acidic residues Asp^{430} and Asp^{436}. When Asp^{430} was replaced with Lys, the resulting D430K mutant was not expressed (Fig. 2). In contrast, when Asp^{436} was replaced with Lys to create D436K, the mutant was expressed but showed a significant decrease in overall organic anion transport activity (Fig. 6 and Table 2). Thus, vesicular uptake by the D436K mutant was decreased by approximately 60% for LTC_4 (Fig. 6A), by 80% for $E_2 17\beta G$ (Fig. 6B), by 70% for $E_1 3SO_4$ (Fig. 6C), by 70% for GSH (Fig. 6D), and by 45% for MTX (Fig. 6E).

Kinetic analyses showed that the apparent K_m (LTC4) of the D436K mutant was increased 2-fold and V_{max} decreased >3-fold, resulting in an overall 7-fold decrease in LTC4 transport efficiency for this mutant (Table 1). Likewise, the apparent K_m ($E_2 17\beta G$) of D436K was increased 3-fold and V_{max} decreased 3-fold, resulting in a 7.5-fold decrease in $E_2 17\beta G$ transport efficiency (Table 3). When the Lys residue in the D436K mutant was replaced with Glu to create the like-charged D(K)436E mutant, wild-type levels of transport activity were observed (Fig. 6, A-E). Kinetic analyses showed that the K_m and V_{max} values for LTC_4 and $E_2 17\beta G$ were also similar to those for wild-type MRP1 (Tables 1 and 3). These data suggest that the charge rather than the volume of the Asp^{436} side chain is the key physical property of this residue required for MRP1 transport activity.

Photolabeling of Wild-Type and Asp^{436} Mutant MRP1 Proteins with $[^3H]LTC_4$. To determine whether the substantially reduced $[^3H]LTC_4$ transport activity of the Asp^{436} mutant D436K was associated with a decrease in substrate binding, photolabeling experiments were carried out with $[^3H]LTC_4$. Photolabeling was also carried out with D(K)436E and wild-type MRP1. As shown in Fig. 6F, $[^3H]LTC_4$ photolabeling of the D436K mutant was reduced by approximately 50% compared with wild-type MRP1. In contrast, photolabeling of the same-charge D(K)436E mutant was similar to wild-type MRP1 as was its LTC_4 transport activity.

Substitution of Asp^{572}, Glu^{573}, Asp^{578}, and Arg^{593} in or near TM11. We next tested the functional importance of three negatively charged amino acids predicted to be in the short fifth extracellular loop between TM10 and TM11 (Asp^{572}, Glu^{573}, and Asp^{578}) and a positively charged amino acid predicted to be in TM11 (Arg^{593}). Asp^{572}, Glu^{573}, and Asp^{578} were substituted with Arg, whereas Arg^{593} was substituted with Glu as well as with the neutral, nonpolar Leu. The D572R, E573R, and D578R mutants exhibited transport activity profiles similar to wild-type MRP1, indicating that none of these negatively charged amino acids are critical for MRP1 transport activity (Table 2). In marked contrast, substitutions of TM11 Arg^{593} with Glu or Leu substantially reduced MRP1 transport activity. As shown in Fig. 7, the LTC_4 (Fig. 7A), GSH (Fig. 7D), and MTX (Fig. 7E) transport activities of the R593E and the R593L mutants were reduced by 70 to 80% relative to wild-type MRP1. In addition, neither mutant transported the conjugated estrogens $E_2 17\beta G$ (Fig. 7B) and $E_1 3SO_4$ (Fig. 7C). Kinetic analysis of LTC_4 transport by the R593E mutant showed that its decreased transport activity was caused by a 4-fold decrease in apparent uptake affinity (K_m = 464 versus 115 nM for wild-type MRP1) and in transport capacity (2-fold decrease in V_{max}), resulting in an overall 10-fold decrease in LTC_4 transport efficiency (Table 1).

To investigate the physical properties of Arg^{593} important for MRP1 transport function, the Glu residue of the R593E mutant was replaced with Lys to create the same-charge mutant R(E)593K. As shown in Fig. 7, A through E, the transport activity of the R(E)593K mutant was comparable with wild-type MRP1 for all five organic anion substrates tested. Kinetic analyses of the R(E)593K mutant also showed that its apparent K_m and V_{max} values for LTC_4 were similar to those of wild-type MRP1 (Table 1). These findings indicate that the charge rather than the size of the Arg^{593} side chain (as was observed for Lys^{396}) is the most critical feature for MRP1 function.

Confocal Microscopy. To determine whether the mutations that caused substantial changes in the transport properties of MRP1 also affected the proper routing of MRP1 to the plasma membrane, the subcellular localization of these mutants was compared with wild-type MRP1 by confocal laser scanning fluorescence microscopy. For these experiments, GFP-tagged constructs encoding wild-type MRP1 and the mutant MRP1 proteins (D336E, K332D/D336K, K396E, D436K, and R593E) were generated and transfected into HEK 293T cells (Koike et al., 2002). When viewed under the confocal microscope, both wild-type and the mutant GFP-tagged MRP1 proteins exhibited an exclusively plasma membrane localization, confirming that they were all correctly routed to the cell surface (Fig. 8).

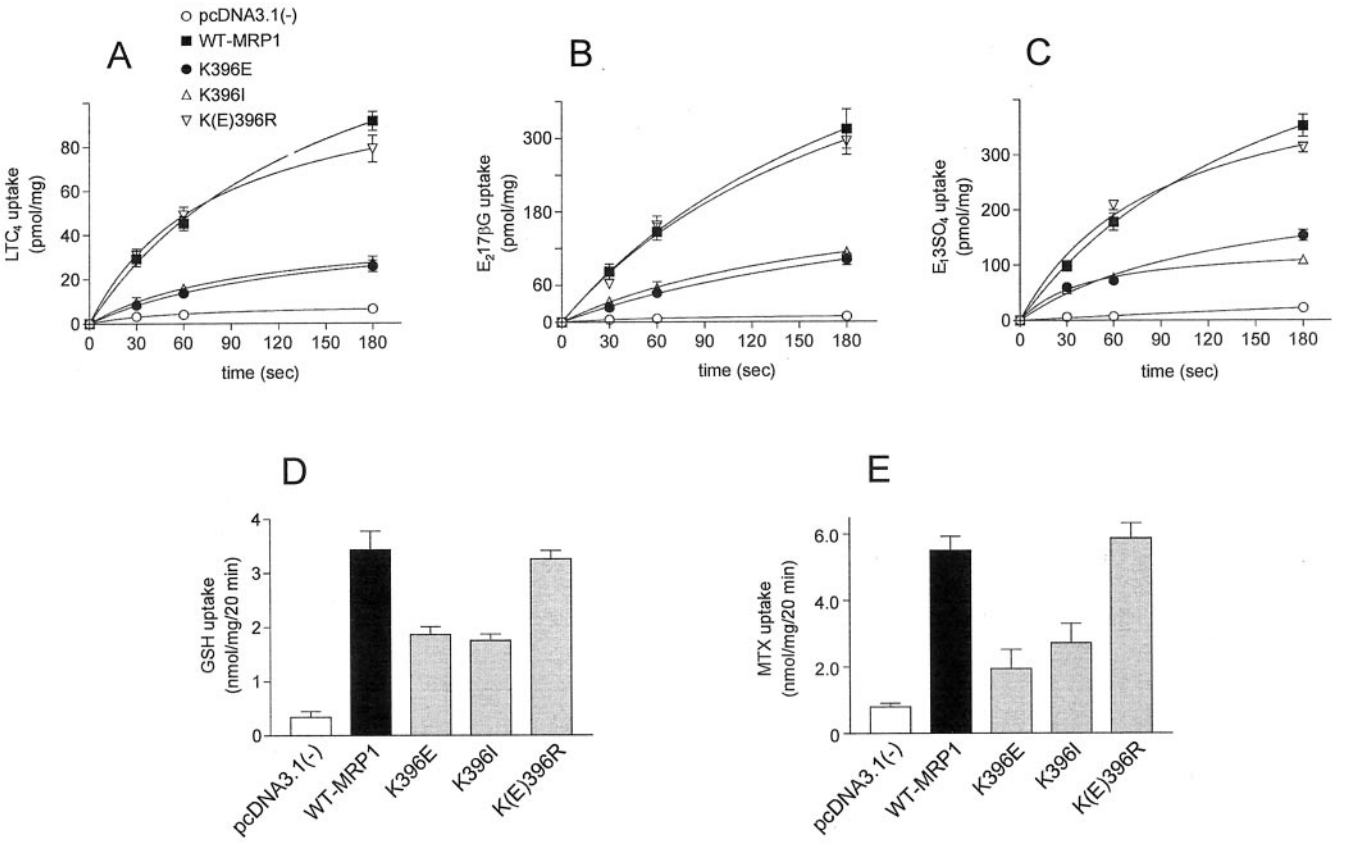

Fig. 5. ATP-dependent ^3H-labeled organic anion uptake into membrane vesicles enriched for MRP1 mutants containing substitutions of Lys^{396}. Time courses of [^3H]LTC_4 uptake (A), [^3H]$E_2 17\beta G$ uptake (B), and GSH-stimulated [^3H]$E_1 3SO_4$ uptake(C) by wild-type (WT) MRP1 (■), mutants K396E (●), K396I (△), and K(E)396R (▽), and empty pcDNA3.1(−) vector control (○). D, apigenin-stimulated [^3H]GSH uptake and [^3H]MTX uptake (E) at 20 min by wild-type MRP1 (■), mutants K396E, K396I, and K(E)396R (▨), and empty pcDNA3.1(−) vector control (□). Results shown are means (± S.D.) of triplicate determinations in a single experiment. Relative MRP1 protein expression levels in the membrane vesicles were as shown in Fig. 2. Similar results were obtained in at least two additional independent experiments.

Discussion

The aims of the present study were 2-fold. The first was to better define the physical properties of TM6 Lys^{332} and Asp^{336} that contribute to the transport activity and substrate specificity of MRP1 (Haimeur et al., 2002). The second was to determine whether any of 11 additional charged amino acids in or proximal to TM6 and the other five TM helices of MSD2 (TM7–TM11) also play a role in organic anion transport by MRP1.

The critical importance of TM6 Lys^{332} as a highly substrate-selective determinant of MRP1 LTC_4 and GSH transport activities was first confirmed by demonstrating that, despite maintaining a positive charge at position 332, transport of LTC_4 and GSH by the K332R mutant remained significantly lower than wild-type MRP1. The reduced LTC_4 transport activity of K332R was associated with a substantial reduction (5-fold) in the apparent LTC_4 uptake affinity (K_m), whereas V_{max} was unchanged. Thus the smaller side chain of an Arg residue cannot fully compensate for the loss of Lys at position 332, indicating that both the volume and charge of the Lys^{332} side chain are critical for LTC_4 binding and transport. This is not the case for other substrates, because the transport of $E_2 17\beta G$, $E_1 3SO_4$ and MTX by the Lys^{332} mutants remained comparable with wild-type MRP1. In a similar way, a like-charge substitution of Glu for Asp at position 336 in the same TM helix of MRP1 resulted in a loss of overall transport activity comparable with that observed with Arg, Lys, or Leu substitutions (Haimeur et al., 2002). Thus, both the charge and volume of the Asp^{336} side chain are also critical for MRP1 transport activity.

We postulated previously that because they are separated by approximately one helical turn from each other, a salt bridge or ion pair critical for maintaining TM6 in a transport-competent configuration might exist between Lys^{332} and Asp^{336}. However, the inactivity of the double-exchange mutant K332D/D336K suggests that this is unlikely to be the case (Fig. 2). It is interesting that both Lys^{332} and Asp^{336} are strictly conserved in MRP1/Mrp1 mammalian orthologs but are only moderately conserved in homologs of the human MRP/ABCC subfamily. Nevertheless, in a study of rat Mrp2,

TABLE 3
Kinetic parameters of $E_2 17\beta G$ uptake by MRP1 MSD2 mutants containing substitutions of Lys^{396} and Asp^{436}

Transfectants	K_m	V_{max}	V_{max}/K_m
	μM	*pmol/mg/min*	$\times 10^3$
Wild-type MRP1	2.6	219	0.9
K396E	4.7	84	0.2
K396(E)R	2.3	195	0.9
D436K	7.7	87	0.1
D(K)436E	2.9	250	0.9

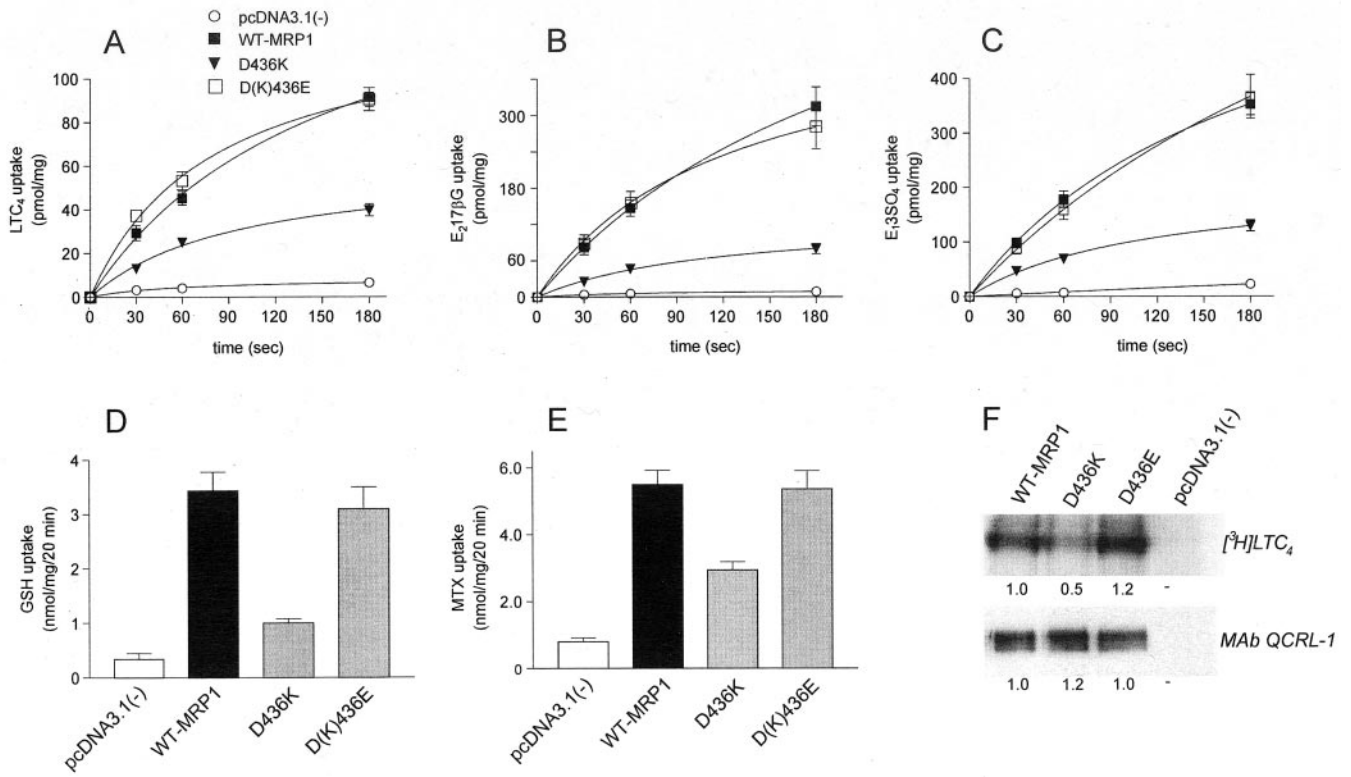

Fig. 6. ATP-dependent uptake of ^3H-labeled organic anions into membrane vesicles enriched for MRP1 mutants containing substitutions of Asp^{436}. Time courses of $[^3H]LTC_4$ uptake (A), $[^3H]E_2 17\beta G$ uptake (B), and GSH-stimulated $[^3H]E_1 3SO_4$ uptake (C) by wild-type MRP1 (■), mutants D436K (▼) and D(K)436E (□), and empty pcDNA3.1(−) vector control (○). D, apigenin-stimulated [^{3}H]GSH uptake and [^{3}H]MTX uptake (E) at 20 min by wild-type MRP1 (■), mutants D436K and D(K)436E (▨), and empty pcDNA3.1(−) vector control (□). Results shown are means (± S.D.) of triplicate determinations in a single experiment. Relative MRP1 protein expression levels in the membrane vesicles were as shown in Fig. 2. Similar results were obtained in at least two additional independent experiments. F, $[^3H]LTC_4$ photolabeling of membrane vesicle proteins prepared from transfected cells. Top, membrane vesicles (50 μg of protein) were incubated with $[^3H]LTC_4$ (0.5 μCi) and then irradiated at 312 nm. Radiolabeled proteins were resolved by SDS-polyacrylamide gel electrophoresis and processed for fluorography. Relative levels of photolabeling were determined by densitometry and are shown below the autoradiograph. Bottom, immunoblot of the membrane vesicles (1 μg of protein) used for the photolabeling experiment shown at the top. MRP1 was detected with MAb QCRL-1, and relative levels of MRP1 were estimated by densitometry and are indicated below the blot. Similar results were obtained in a second set of experiments.

mutational analyses of the analogous Lys^{325} and Asp^{329} residues showed that they too could not be functionally replaced with like-charge amino acids (Ito et al., 2001b).

Nonconservative substitutions of two other positively charged Lys residues at positions 319 and 347 NH_2- and COOH-proximal to TM6, respectively, had little effect except to cause a moderate and selective reduction in GSH transport by MRP1. On the other hand, GSH-stimulated E_13SO_4 transport by the Lys^{319} and Lys^{347} mutants was comparable with wild-type MRP1. These observations suggest that the mutations affected the transport rather than the binding of GSH because cotransport of GSH is not required to stimulate E_13SO_4 transport by MRP1. Taken together, our observations are consistent with the conclusion that the TM6 region of MSD2 has a particularly important role in GSH transport by MRP1.

In addition to the four charged residues in or proximal to TM6 discussed above, MSD2 contains nine charged amino acids that, according to several topological models developed using common computer algorithms, are predicted to be located in or proximal to TM7 to TM11 (Hipfner et al., 1997). When these residues were replaced with oppositely charged amino acids, all but one of the resulting mutants could be expressed. The exception was the Asp^{430} mutant D430K. Northern blot analyses showed that the D430K-expressing cells contained levels of the mutant *MRP1* mRNA that were comparable with those of wild-type *MRP1* transfected cells, indicating a post-transcriptional event is probably involved (results not shown).

Of the eight other charged amino acids in TM7 to TM11 examined, only the oppositely charged mutants of Lys^{396}, Asp^{436}, and Arg^{593} showed major changes in transport activity. Thus, despite the close proximity of Arg^{394} and Lys^{396} to one another, mutation of Arg^{394} to an oppositely charged amino acid had no effect, whereas a similar substitution of Lys^{396} caused a substantial and global loss of transport activity. These two basic residues are both relatively well-conserved in other ABCC family members but are predicted to be on opposite faces of an α-helix that extends through the membrane as TM8 well into the cytoplasm (Campbell et al., 2004). Consequently, they would differ in their accessibility for interactions with other regions of MRP1 that are believed to occur during substrate binding and translocation. Whether or not differences in the relative accessibility of Arg^{394} and Lys^{396} are related to the differences in their functional importance for MRP1 transport activity is not yet known.

Unlike the oppositely charged mutant of Asp^{430} discussed earlier, the TM8 D436K mutant was expressed at levels comparable with those of wild-type MRP1. However, the transport activity of this mutant was substantially reduced. Two other Asp residues shown to be important for overall MRP1 transport activity include the previously discussed

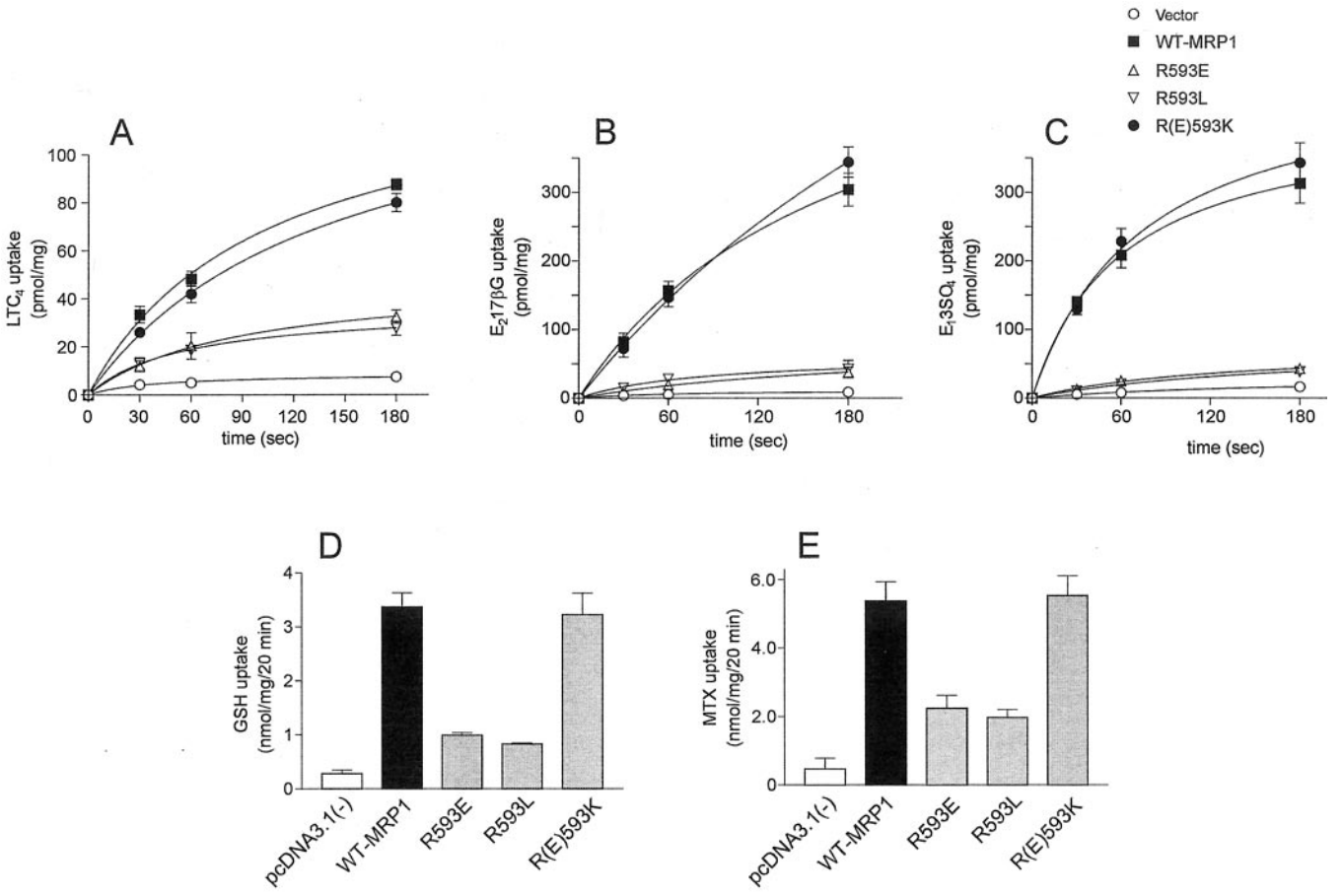

Fig. 7. ATP-dependent uptake of ^{3}H-labeled organic anions into membrane vesicles enriched for MRP1 mutants containing substitutions of TM11 Arg^{593}. Time courses of [^{3}H]LTC_4 uptake (A), [^{3}H]$E_217\beta G$ uptake (B), and GSH-stimulated [^{3}H]E_13SO_4 uptake (C) by wild-type MRP1 (■), mutants R593E (△), R593L (▽), and R(E)593K (●), and empty pcDNA3.1(−) vector control (○). D, apigenin-stimulated [^{3}H]GSH uptake and [^{3}H]MTX uptake (E) at 20 min by wild-type (WT) MRP1 (■), mutants R593E, R593L, and R(E)593K (▨), and empty pcDNA3.1(−) vector control (□). Results shown are means (± S.D.) of triplicate determinations in a single experiment. Relative MRP1 protein expression levels in the membrane vesicles were as shown in Fig. 2. Similar results were obtained in at least two additional independent experiments.

Asp^{336} in TM6 (Haimeur et al., 2002) and Asp^{1084} proximal to the cytoplasmic end of TM14 in MSD3 (Zhang et al., 2003) (D. Situ, A. Haimeur, G. Conseil, K. E. Sparks, D. Zhang, R. G. Deeley, S. P. C. Cole, manuscript in preparation). Despite a comparable loss of transport activity, nonconservative mutations of Asp^{336} completely abrogated [^{3}H]LTC_4 photolabeling, whereas similar mutations of Asp^{1084} had no effect. In the present study, the reduced transport activity of the D436K mutant was associated with reduced LTC_4 binding, and in this way, the D436K mutant is more similar to the Asp^{336} mutants than to the Asp^{1084} mutants described previously.

Opposite-charge substitutions of either Lys^{396} or Asp^{436} substantially reduced transport activity, although the global structure of MRP1 was not severely disrupted because the K396E and D436K mutants retained some low level of activity. This allowed us to determine the kinetic parameters of LTC_4 and $E_217\beta G$ transport, which revealed that significant changes in both the apparent K_m and V_{max} for these substrates had occurred. It is interesting that reintroducing conservative substitutions of Lys^{396} and Asp^{436} [as in K(E)396R and D(K)436E], re-established wild-type transport activity, indicating that the charges of the side chains, rather than their molecular volumes, are the most important property of these amino acids for MRP1 transport function. These findings contrast with those for TM6 Asp^{336}, in which the transport activity of the same-charge D(K)336E mutant remained very low.

Substitutions of Arg^{593} (TM11) resulted in a somewhat different phenotype from those observed for the Lys^{332}, Asp^{336}, Lys^{396}, and Asp^{436} mutants. Thus, the nonconservatively substituted R593E and R593L mutants displayed a complete loss of $E_217\beta G$ and E_13SO_4 transport and a substantial loss of LTC_4, GSH, and MTX transport. On the other hand, the like-charge substitution of Arg^{593} with Lys resulted in a fully functional MRP1 R(E)593K. This indicates that a positive charge at position 593 in TM11 is sufficient for MRP1 function, and changes in the side chain volume seem less important. It is interesting that transport activity was also retained when the analogous Arg^{586} residue of rat Mrp2 was replaced with Lys but not when replaced with Leu, although it should be noted that only a limited number of substrates were tested in this latter study (Ito et al., 2001b).

It is not known at present whether TM11 Arg^{593}, which is in the inner leaflet of the membrane bilayer, plays a structural or dynamic role, or both. However, the lack of LTC_4 binding by R593E and the global reduction in its transport activity indicates that Arg^{593} is important for high-affinity binding of LTC_4 and presumably other substrates as well. It is also clear that this region of TM11 is particularly critical for MRP1 transport activity because we have shown recently that nonconservative substitutions of either of the nearby Phe^{594} or Pro^{595} also result in a global loss of organic anion transport and LTC_4 binding (Campbell et al., 2004; Koike et al., 2004). Major photoaffinity drug binding sites have also been identified in a proteolytic

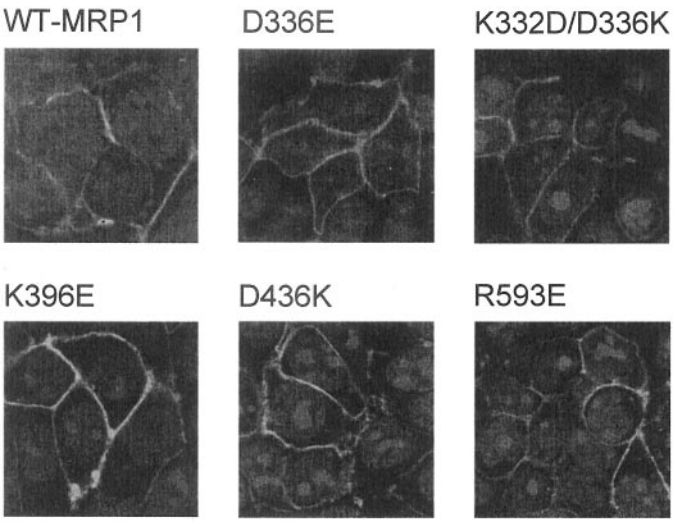

Fig. 8. Confocal laser scanning fluorescence micrographs of transfected HEK 293T cells expressing GFP-tagged wild-type and MSD2 mutant MRP1 cDNA constructs. The subcellular localization of wild-type and selected MSD2 mutant MRP1 cDNA constructs was determined by confocal microscopy (Haimeur et al., 2002). HEK 293T cells were transfected with the wild-type pcDNA3.1(−)-MRP1-GFP and mutant pcDNA3.1(−)-MRP1-D336E-GFP, pcDNA3.1(−)-MRP1-K332D/D336K-GFP, pcDNA3.1(−)-MRP1-K396E-GFP, pcDNA3.1(−)-MRP1-D436K-GFP, and pcDNA3.1(−)-MRP1-R593E-GFP expression vectors as indicated, and cells were viewed 48 h later under the confocal microscope. GFP signals were collected with a 530/30-nm bandpass filter. Nuclei were stained with propidium iodide, and signals were collected with a 600/40-nm bandpass filter.

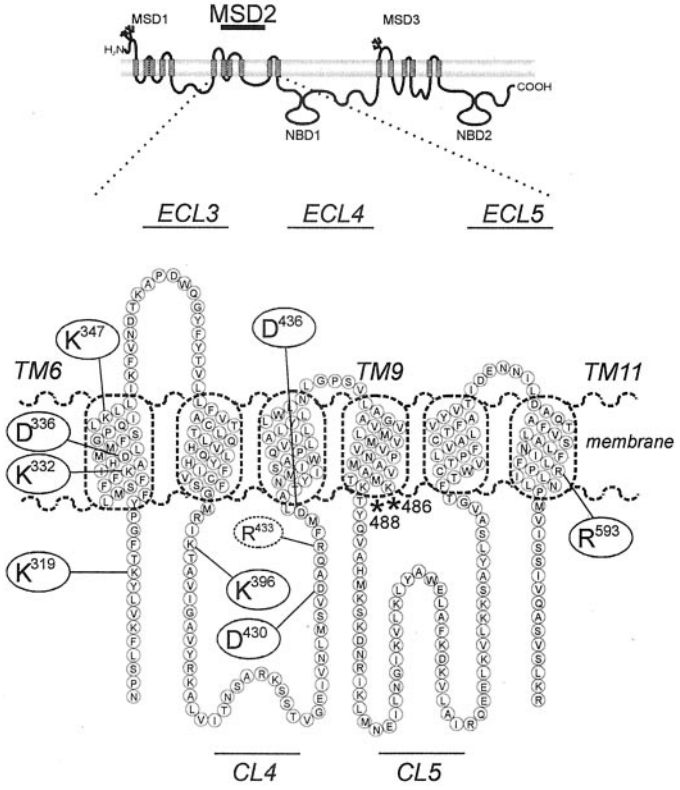

Fig. 9. Topological model of MRP1 MSD2 based on crystal structures of the bacterial lipid transporter MsbA. A schematic diagram of MSD2 of MRP1 shows the approximate boundaries of TM6 to TM11 derived from the crystal structure of the *Vibrio cholerae* lipid transporter MsbA and an energy-minimized P-glycoprotein simulation (Campbell et al., 2004). The locations of the charged amino acids in and proximal to MSD2 that were demonstrated in this study to be important for MRP1 expression, transport activity, and/or substrate specificity are indicated. The naturally occurring Arg^{433}→Ser MRP1 mutant was characterized by Conrad et al. (2002). Also indicated by two asterisks are Lys^{486} and Lys^{488} that are predicted by the *V. cholerae* MsbA-based model of MRP1 MSD2 to be proximal to the TM9-cytosol interface, whereas hydropathy-based topology algorithms predict them to be located well into cytoplasmic loop 5. ECL, extracellular loop; CL, cytoplasmic loop.

fragment of MRP1 that encompasses TM10 and TM11 (Ser^{542} to Arg^{593}) (Daoud et al., 2001).

There is presently little direct experimental evidence defining the boundaries and interhelical packing interactions of the 17 TM helices of MRP1 or how they are modified during a cycle of substrate binding and transport that is coupled to nucleotide binding and hydrolysis. We recently developed models of MSD2 and MSD3 of MRP1 that are derived from the crystal structures of two bacterial MsbA lipid transporters and a P-glycoprotein simulation (Campbell et al., 2003, 2004; Stenham et al., 2003). According to our models, TM6 Lys^{332} and Asp^{336} are in the inner leaflet of the membrane facing in toward a pore or chamber through which substrates are presumed to be translocated (Fig. 9). Likewise, Asp^{436} at the TM8-cytosol interface and Arg^{593} in the inner leaflet of TM11 (Fig. 9) line the pore or substrate translocation pathway of MRP1 (Campbell et al., 2004). Lys^{396} at the TM7-cytosol interface could also face inward, although the predicted position of this residue is more variable in other models of MSD2. Overall, however, the locations of these five charged residues predicted by our model are consistent with their demonstrated importance as determinants of MRP1 transport activity and substrate specificity.

Unlike the hydropathy-based TM-predicting algorithm of Eisenberg et al. (1984), our crystal-based models of MSD2 place two additional charged residues, Lys^{486} and Lys^{488}, at the membrane-cytosol interface of TM9 (Fig. 9). However, the side chains of these residues face outward from the putative translocation pathway of MRP1 (Campbell et al., 2004). As might be predicted with such a location, nonconservative mutations of Lys^{486} and Lys^{488} had no significant effect on MRP1 transport activity (results not shown).

Finally, it is interesting to note that the amino acid analogous to Arg^{593} in CFTR is Arg^{347}, and there is evidence for the existence of a salt bridge between this residue and Asp^{924} in the COOH-proximal MSD that is important for CFTR function (Cotten and Welsh, 1999). CFTR-Asp^{924} is not conserved in MRP1; instead, a polar residue, Gln^{1026}, is found at the analogous position in TM13 of MSD3. Whether or not MRP1-Arg^{593} interacts with Gln^{1026} via hydrogen bonding or interacts with an acidic or polar residue elsewhere in MSD3, or neither, is currently under investigation. Characterization of the interhelical bonding interactions of other functionally important charged residues we have identified with either charged or polar residues is also the subject of ongoing studies.

Acknowledgments

We thank Christophe Moreau (Queen's University) and Jeff Campbell (University of Oxford, United Kingdom) for helpful discussions and advice. We thank Maureen Rogers for expert word processing and assistance in the preparation of the figures.

References

Borst P, Evers R, Kool M, and Wijnholds J (2000) A family of drug transporters: the multidrug resistance-associated proteins. *J Natl Cancer Inst* **92:**1295–1302.

Campbell JD, Biggin PC, Baaden M, and Sansom MSP (2003) Extending the structure of an ABC transporter to atomic resolution: modeling and simulation studies of MsbA. *Biochemistry* **42:**3666–3673.

Campbell JD, Koike K, Moreau C, Sansom MS, Deeley RG, and Cole SP (2004) Molecular modeling correctly predicts the functional importance of Phe^{594} in transmembrane helix 11 of the multidrug resistance protein, MRP1 (ABCC1). *J Biol Chem* **279:**463–468.

Conrad S, Kauffmann H-M, Ito K, Leslie EM, Deeley RG, Schrenk D, and Cole SPC (2002) A naturally occurring mutation in MRP1 results in a selective decrease in organic anion transport and in increased doxorubicin resistance. *Pharmacogenetics* **12:**321–330.

Cotten JF and Welsh MJ (1999) Cystic fibrosis-associated mutations at arginine 347 alter the pore architecture of CFTR. *J Biol Chem* **274:**5429–5435.

Daoud R, Julien M, Gros P, and Georges E (2001) Major photoaffinity drug binding sites in MRP1 are within TM10–11 and TM16–17. *J Biol Chem* **276:**12324–12330.

de Jong MC, Slootstra JW, Scheffer GL, Schroeijers AB, Puijk WC, Dinkelberg R, Kool M, Broxterman HJ, Meloen RH, and Scheper RJ (2001) Peptide transport by the multidrug resistance protein MRP1. *Cancer Res* **61:**2552–2557.

Deeley RG and Cole SPC (2003) Multidrug resistance protein 1 (ABCC1), in *ABC Proteins: from Bacteria to Man* (Holland IB, Cole SPC, Kuchler K, and Higgins CF eds) pp 393–422, Elsevier Science, London.

Eisenberg D, Schwarz E, Komaromy M, and Wall R (1984) Analysis of membrane and surface protein sequences with the hydrophobic moment plot. *J Mol Biol* **179:**125–142.

Haimeur A, Conseil G, Deeley RG, and Cole SPC (2004) The MRP-related and BCRP/ABCG2 multidrug resistance proteins: biology, substrate specificity and regulation. *Curr Drug Metab* **5:**21–53.

Haimeur A, Deeley RG, and Cole SPC (2002) Charged amino acids in the sixth transmembrane helix of multidrug resistance protein 1 (MRP1/ABCC1) are critical determinants of transport activity. *J Biol Chem* **277:**41326–41333.

Higgins CF (1992) ABC transporters: from microorganisms to man. *Ann Rev Cell Biol* **8:**67–113.

Hipfner DR, Almquist KC, Leslie EM, Gerlach JH, Grant CE, Deeley RG, and Cole SPC (1997) Membrane topology of the multidrug resistance protein, MRP: a study of glycosylation-site mutants reveals an extracytosolic NH_2-terminus. *J Biol Chem* **272:**23623–23630.

Hipfner DR, Almquist KC, Stride BD, Deeley RG, and Cole SPC (1996) Location of a protease-hypersensitive region in the multidrug resistance protein (MRP) by mapping of the epitope of MRP-specific monoclonal antibody QCRL-1. *Cancer Res* **56:**3307–3314.

Ito K, Olsen SL, Qiu W, Deeley RG, and Cole SPC (2001a) Mutation of a single conserved tryptophan in multidrug resistance protein 1 (MRP1/ABCC1) results in loss of drug resistance and selective loss of organic anion transport. *J Biol Chem* **276:**15616–15624.

Ito K, Suzuki H, and Sugiyama Y (2001b) Charged amino acids in the transmembrane domains are involved in the determination of the substrate specificity of rat Mrp2. *Mol Pharmacol* **59:**1077–1085.

Koike K, Conseil G, Leslie EM, Deeley RG, and Cole SPC (2004) Identification of proline residues in the core cytoplasmic and transmembrane regions of multidrug resistance protein 1 (MRP1/ABCC1) important for transport function, substrate specificity and nucleotide interactions. *J Biol Chem*, in press.

Koike K, Oleschuk CJ, Haimeur A, Olsen SL, Deeley RG, and Cole SPC (2002) Multiple membrane associated tryptophan residues contribute to the transport activity and substrate specificity of the multidrug resistance protein, MRP1. *J Biol Chem* **277:**49495–49503.

Konig J, Nies AT, Cui Y, and Keppler D (2003) MRP2, the apical export pump for anionic conjugates, in *ABC Transporters: from Bacteria to Man* (Holland IB, Cole SPC, Kuchler K, and Higgins CF eds) pp 423–443, Elsevier Science, London.

Leslie EM, Deeley RG, and Cole SPC (2003a) Bioflavonoid stimulation of glutathione transport by the 190-kDa multidrug resistance protein 1 (MRP1). *Drug Metab Dispos* **31:**11–15.

Leslie EM, Letourneau IJ, Deeley RG, and Cole SPC (2003b) Functional and structural consequences of cysteine substitutions in the NH_2-proximal region of the human multidrug resistance protein 1 (MRP1/ABCC1). *Biochemistry* **42:**5214–5224.

Loe DW, Almquist KC, Deeley RG, and Cole SPC (1996) Multidrug resistance protein (MRP)-mediated transport of leukotriene C_4 and chemotherapeutic agents in membrane vesicles: demonstration of glutathione-dependent vincristine transport. *J Biol Chem* **271:**9675–9682.

Loe DW, Deeley RG, and Cole SPC (1998) Characterization of vincristine transport by the 190 kDa multidrug resistance protein, MRP: evidence for co-transport with reduced glutathione. *Cancer Res* **58:**5130–5136.

Mao Q, Deeley RG, and Cole SPC (2000) Functional reconstitution of substrate transport by purified multidrug resistance protein MRP1 (ABCC1) in phospholipid vesicles. *J Biol Chem* **275:**34165–34172.

Raab-Graham KF, Cirilo LJ, Boettcher AA, Radeke CM, and Vandenberg CA (1999) Membrane topology of the amino-terminal region of the sulfonylurea receptor. *J Biol Chem* **274:**29122–29129.

Rost B, Fariselli P, and Casadio R (1996) Topology prediction for helical transmembrane proteins at 86% accuracy. *Protein Sci* **5:**1704–1718.

Stenham DR, Campbell JD, Sansom MSP, Higgins CF, Kerr ID, and Linton KJ (2003) An atomic detail model for the human ATP-binding cassette transporter P-glycoprotein derived from disulphide cross-linking and homology modeling. *FASEB J* **17:**2287–2289.

Yang Y, Chen Q, and Zhang J-T (2002) Structural and functional consequences of mutating cysteine residues in the amino terminus of human multidrug resistance-associated protein 1. *J Biol Chem* **277:**44268–44277.

Zhang D, Cole SPC, and Deeley RG (2001) Identification of an amino acid residue in multidrug resistance protein (MRP) 1 critical for conferring resistance to anthracyclines. *J Biol Chem* **276:**13231–13239.

Zhang D, Cole SPC, and Deeley RG (2002) Determinants of the substrate binding specificity of multidrug resistance protein (MRP1): role of amino acid residues with hydrogen bonding potential in predicted transmembrane helix 17. *J Biol Chem* **277:**20934–20941.

Zhang D, Gu H, Situ D, Haimeur A, Cole SPC, and Deeley RG (2003) Functional importance of polar and charged amino acid residues in transmembrane helix 14 of multidrug resistance protein 1 (MRP1/ABCC1): identification of an aspartate residue critical for conversion from a high to low affinity substrate binding site. *J Biol Chem* **278:**46052–46063.

Address correspondence to: Dr. Susan P. C. Cole, Cancer Research Laboratories, 3rd Floor, Botterell Hall, Queen's University, Kingston, Ontario K7L 3N6 Canada. E-mail: coles@post.queensu.ca